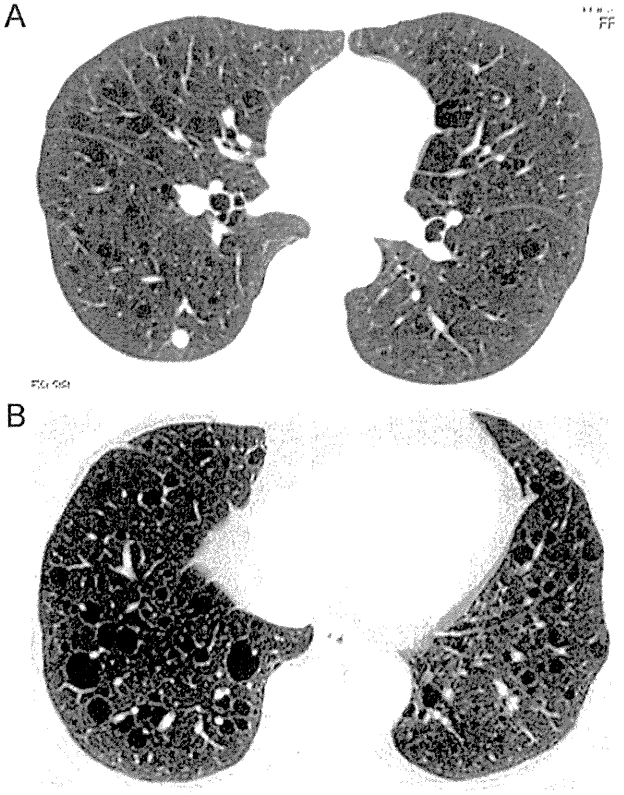

Fig. 1 – Chest computed tomography in cases 1 (A) and 2 (B), showing a small nodule in the right lower lobe (A) and bilateral multiple thin-walled cysts (A, B).

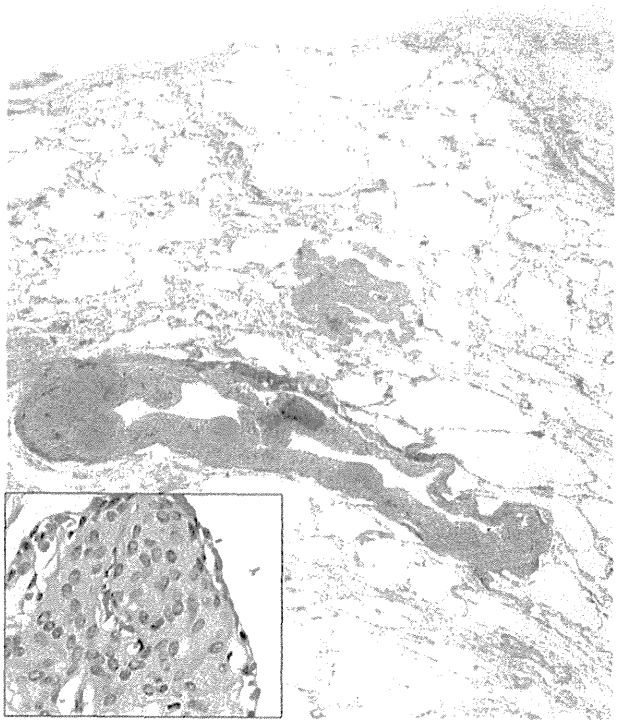

Fig. 2 – The microscopic findings related to the surgically biopsied specimen in case 1 (hematoxylin and eosin stain) showing some cyst-like spaces, mildly thickened alveolar walls, and nodular lesions. Focal proliferations of short spindle-shaped cells were present (inset).

findings of the skin; chest auscultation and SpO_2 measurements were also normal. The laboratory findings showed no abnormal data, and no α1-antitripsin deficiency was found. No abnormal findings were detected on chest radiography. Pulmonary function tests revealed a vital capacity (VC) of 2.94 L (106.5% predicted), a forced expiratory volume in one second ($FEV_{1.0}$) of 2.17 L, an $FEV_{1.0\%}$ of 81.9%, and a percent diffusion lung capacity for carbon monoxide ($\%D_{LCO}$) of 71.3%. A surgical lung biopsy was performed, and the small nodule in the right lower lobe was diagnosed as an intrapulmonary lymph node.

Immunohistochemical staining of the lung specimen (Fig. 2) was positive for α-smooth muscle actin, HMB45, the estrogen receptor, and the progesterone receptor (data not shown). Therefore, the patient was diagnosed with pulmonary LAM. Findings of tuberous sclerosis were not observed in other organs. Thus far, we have not been able to obtain permission from the patient for tumor suppressor gene (tuberous sclerosis complex; TSC) testing. In the 3 years that have elapsed since the patient's diagnosis, pulmonary function tests and chest CT findings have shown no deterioration.

2.2. *Case 2*

A 66-year-old Japanese woman without any respiratory symptoms was referred because of multiple lung cysts (Fig. 1B) that had been discovered on chest CT performed for a general check-up before surgery for dermatofibrosarcoma protuberans of the neck. The patient had reached menopause at age 52, and was never prescribed estrogen replacement therapy. At age 58, she underwent hysterectomy and oophorectomy for treatment of uterine cancer with simultaneous resection of a renal tumor. The resected tissue was pathologically diagnosed as renal angiomyolipoma. She had never smoked or inhaled any toxic materials. No past or family history of spontaneous pneumothorax was reported. Physical and laboratory examinations showed normal results. The patient's chest radiography showed normal results. Pulmonary function tests revealed a VC of 1.92 L (83.8% predicted), $FEV_{1.0}$ of 1.30 L, $FEV_{1.0\%}$ of 75.1%, and $\%D_{LCO}$ of 62.0%. No findings of tuberous sclerosis were observed. Unfortunately, we have not been able to obtain permission from the patient or family for TSC genetic testing. Although no lung biopsy was performed for confirmation, the patient did not show characteristics of other diseases that can cause pulmonary cysts, such as pulmonary emphysema, Langerhans' cell histiocytosis, and Sjogren's syndrome. The patient met the diagnostic criteria [2] for LAM with renal angiomyolipoma. There has been no deterioration detected by pulmonary function tests or chest CT findings during the 2 years since the diagnosis.

3. Discussion

We herein presented two cases of LAM that developed after gynecological surgery in postmenopausal women who had not taken any estrogen hormone replacement therapy.

Neither of the patients had progressive dyspnea nor repeated spontaneous pneumothorax, and there was a possibility that the onset of LAM had occurred after menopause in both cases. The previous [3-13] and present reports of 15 postmenopausal patients with pulmonary LAM (mean age of onset; 62.7 years) (Table 1) showed that eight patients underwent gynecological surgery (hysterectomy and/or oophorectomy, salpingectomy), while the others experienced natural menopause. Five of the 15 patients had received estrogen hormone replacement therapy after menopause (Cases 5, 6, 8, 9, and 12). Three patients were treated for LAM with progesterone or tamoxifen (Cases 7-9). When compared to the patients who did not receive treatment, these cases exhibited slight improvements in pulmonary function and arterial oxygen tension and had prolonged survival. In contrast, six patients, including the two cases presented here, remained stable in terms of CT findings and pulmonary function, without any treatment. Thus, the effects of anti-estrogenic therapy among these 15 patients are controversial.

Seyama et al. reported that five of 11 premenopausal patients with pulmonary LAM who had not received anti-hormone therapy showed slower progression of the cystic changes on CT and pulmonary function tests, which was not the case for the six patients who had received anti-hormone therapy [14]. Furthermore, one large study of patients with LAM showed no benefit of treatment in terms of the decline in lung function [15]. Therefore, we think that anti-estrogenic therapy may not always be necessary for LAM patients, especially those in whom disease onset occurs after menopause, and who exhibit a stable course without any hormone-related therapy.

The etiology of LAM is still unclear. LAM cells in the lungs are immunohistochemically positive for estrogen and progesterone receptors, and usually are limited to the large epithelioid cells, but there is no evidence that individuals with estrogen receptor-positive pulmonary LAM tend to respond to anti-estrogenic therapy. In most patients with pulmonary LAM, the LAM cells contain somatic mutations of the TSCs. The *TSC1* gene is located at 9q34 and encodes the hamartin protein, while *TSC2* is located at 16p13.3 and encodes tuberin [16]. *TSC1* and *TSC2* form a heterodimer complex, where hamartin is the regulatory component stabilizing tuberin. Deficiencies or dysfunction of either hamartin or tuberin activate the mammalian target of rapamycin (mTOR) and other downstream proteins, resulting in increased protein translation and inappropriate cellular proliferation [17]. The TSC1/TSC2-related signaling pathways are also involved in the pathogenesis of pulmonary LAM. Currently, it is thought that both sporadic pulmonary LAM and pulmonary LAM associated with the tuberous sclerosis complex occur via a two-hit mechanism with a mutation of either the *TSC2* or *TSC1* gene, followed by a second hit leading to a loss of heterozygosity, causing the loss of function of either protein. However, no model of pulmonary LAM cells is available thus far, and the relative contributions of *TSC1*/*TSC2* have not been clarified. On the other hand, sporadic cases of pulmonary LAM show a *TSC2* mutation predominance, and it was reported that the size of lung cysts did not differ in tuberous sclerosis patients with either the *TSC1* or *TSC2* mutation, while patients with *TSC2* mutations had more cysts than patients with *TSC1* mutations [18]. Another study [19] demonstrated that tuberous sclerosis patients with *TSC1* mutations had, on average, milder disease than those with *TSC2* mutations. Linking the distribution and types of *TSC1* or *TSC2* mutations with a specific gene region may affect treatment decisions and prognostic determinations. Considering these facts and the instances of LAM observed in postmenopausal women, we believe that excess estrogen and progesterone deficiency are not the primary causes of the disease, but may be one of the triggers for pulmonary LAM progression. Recent therapeutic trials with sirolimus, an inhibitor of mTOR, have shown stabilized lung function associated with a reduction in symptoms and improvement in the quality of life [20]. However, the indications for sirolimus treatment for LAM in postmenopausal women currently remain unknown.

Further studies on the role of TSC are needed to elucidate the relationships with the age of onset and/or the degree of LAM progression. Clinicians should be aware of the potential for pulmonary LAM in the differential diagnosis of pulmonary

Table 1 – Reported postmenopausal cases of pulmonary lymphangioleiomyomatosis.

	Year	Age	History of surgery	Estrogen replacement	Symptom	Treatment	Outcome
1 [3]	1964	69	(−)	(−)	Dyspnea	(−)	N.D.
2 [4]	1973	65	Salpingectomy	(−)	Dyspnea	(−)	Died
3 [5]	1980	70	(−)	(−)	Dyspnea	(−)	Survived
4 [6]	1985	72	Hysterectomy	(−)	Dyspnea	(−)	Died
5 [7]	1990	49	Hysterectomy, oophorectomy	(+)	N.D.	N.D.	N.D.
6 [7]		61	Hysterectomy, oophorectomy	(+)	N.D.	N.D.	N.D.
7 [8]	1994	59	(−)	(−)	Dyspnea	Tamoxifen	Survived
8 [8]		62	Hysterectomy, oophorectomy	(+)	Dyspnea	Progesterone	Survived
9 [9]	1996	62	(−)	(+)	Dyspnea	Progesterone	Survived
10 [10]	2001	75	(−)	(−)	(−)	(−)	Unknown
11 [11]	2007	59	(−)	(−)	(−)	N.D.	N.D.
12[12]	2009	51	Hysterectomy, oophorectomy	(+)	(−)	(−)	Survived
13 [13]	2010	70	(−)	(−)	Dyspnea	N.D.	N.D.
Present cases		50	Hysterectomy	(−)	(−)	(−)	Survived
		66	Hysterectomy, oophorectomy	(−)	(−)	(−)	Survived

N.D.: not described.

cystic diseases, and should consider LAM even in elderly patients. More postmenopausal cases of LAM should be reviewed to determine the proper treatment and help elucidate the pathogenesis of the disease.

Conflict of interest

The authors have no conflicts of interest.

REFERENCES

[1] Seyama K, Kumasaka T, Kurihara M, et al. Lymphangioleiomyomatosis: a disease involving the lymphatic system. Lymphat Res Biol 2010;8:21–31.

[2] Hayashida M, Seyama K, Inoue Y, et al. Criteria for designation of lymphangioleiomyomatosis in the Specified Disease Treatment Research Program. Nihon Kokyuki Gakkai Zasshi 2011;49:67–74 ([in Japanese, abstract in English]).

[3] Rienhoff III WF, Shelley WM, Cornell WP. Lymphangiomatous malformation of thoracic duct associated with chylous pleural effusion. Ann Surg 1964;159:180–4.

[4] Joliat G, Stalder H, Kapanci Y. Lymphangiomyomatosis: a clinico-anatomical entity. Cancer 1973;31:455–61.

[5] Bradley SL, Dines DE, Soule EH, et al. Pulmonary lymphangiomyomatosis. Lung 1980;158:69–80.

[6] Sinclair W, Wright JL, Churg A. Lymphangioleiomyomatosis presenting in a postmenopausal woman. Thorax 1985;40:475–6.

[7] Taylor JR, Ryu J, Colby TV, et al. Lymphangioleiomyomatosis. Clinical course in 32 patients. N Engl J Med 1990;323:1254–60.

[8] Baldi S, Papotti M, Valente ML, et al. Pulmonary lymphangioleiomyomatosis in postmenopausal women: report of two cases and review of the literature. Eur Respir J 1994;7:1013–6.

[9] Zanella A, Toppan P, Nitti D, et al. Pulmonary lymphangioleiomyomatosis: a case report in postmenopausal woman treated with pleurodesis and progesterone (medroxyprogesterone acetate). Tumori 1996;82:96–8.

[10] Matsushima H, Takayanagi N, Kawata I, et al. A case of pulmonary lymphangioleiomyomatosis in an elderly woman. Nihon Kokyuki Gakkai Zasshi 2001;39:519–23 ([in Japanese, abstract in English]).

[11] Pollock-BarZiv S, Cohen MM, Downey GP, et al. Air travel in women with lymphangioleiomyomatosis. Thorax 2007;62:176–80.

[12] Borovansky JA, Labonte HR, Boroff ES, et al. Lymphangioleiomyomatosis: a case report. J Womens Health (Larchmt) 2009;18:535–8.

[13] Soler-Ferrer C, Gomez-Lozano A, Clemente-Andres C, et al. Lymphangioleiomyomatosis in a post-menopausal women. Arch Bronconeumol 2010;46:148–50 ([in Spanish, abstract in English]).

[14] Seyama K, Kira S, Takahashi H, et al. Longitudinal follow-up study of 11 patients with pulmonary lymphangioleiomyomatosis: diverse clinical courses of LAM allow some patients to be treated without anti-hormone therapy. Respirology 2001;6:331–40.

[15] Johnson SR. Lymphangioleiomyomatosis. Eur Respir J 2006;27:1056–65.

[16] Krymskaya VP. Smooth muscle-like cells in pulmonary lymphangioleiomyomatosis. Proc Am Thorac Soc 2008;5:119–26.

[17] Chorianopoulos D, Stratakos G. Lymphangioleiomyomatosis and tuberous sclerosis complex. Lung 2008;186:197–207.

[18] Sancak O, Nellist M, Goedbloed M, et al. Mutational analysis of the TSC1 and TSC2 genes in a diagnostic setting: genotype–phenotype correlations and comparison of diagnostic DNA techniques in Tuberous Sclerosis Complex. Eur J Hum Genet 2005;13:731–41.

[19] Dabora SL, Jozwiak S, Franz DN, et al. Mutational analysis in a cohort of 224 tuberous sclerosis patients indicates increased severity of TSC2, compared with TSC1, disease in multiple organs. Am J Hum Genet 2001;68:64–80.

[20] McCormack FX, Inoue Y, Moss J, et al. Efficacy and safety of sirolimus in lymphangioleiomyomatosis. N Engl J Med 2011;364:1595–606.

Contents lists available at ScienceDirect

Respiratory Investigation

journal homepage: www.elsevier.com/locate/resinv

Short Communication

Chest computed tomography findings in patients with angioimmunoblastic T-cell lymphoma

Hiroshi Ishii, M.D.[a,b,*], *Hisako Kushima*[a], *Kosaku Komiya*[a], *Fumito Okada*[c], *Kentaro Watanabe*[b], *Jun-ichi Kadota*[a]

[a]*Department of Respiratory Medicine, Oita University Hospital, Hasama-machi, Oita 879-5593, Japan*
[b]*Department of Respiratory Medicine, Fukuoka University Hospital, 7-45-1 Nanakuma, Fukuoka-city, Fukuoka 814-0180, Japan*
[c]*Department of Radiology, Oita University Hospital, Hasama-machi, Oita 879-5593, Japan*

ARTICLE INFO

Article history:
Received 30 July 2013
Received in revised form
16 January 2014
Accepted 19 January 2014
Available online 14 February 2014

Angioimmunoblastic T-cell lymphoma (AITL) is a rare and aggressive (fast-growing) neoplasm that occurs in elderly individuals. AITL accounts for 1–2% of all non-Hodgkin lymphoma cases. It is a systemic lymphoproliferative disorder characterized by sudden onset of constitutional symptoms, generalized lymphadenopathy, hepatosplenomegaly, rashes, anemia, frequent autoimmune phenomena, and polyclonal hypergammaglobulinemia [1,2]. As a result of these autoimmune disorders, the body's immune system does not recognize and consequently destroys its own cells and tissues [2]. The median age of patients with AITL is 60–65 years, with an equal incidence among men and women [3]. On diagnosis, the majority of patients present with advanced stage disease and a poor prognosis associated with conventional treatment, with a median overall survival of less than three years. Histologically, the normal architecture of the lymph node is effaced by polymorphic cellular infiltrates composed of lymphocytes, plasma cells, eosinophils, histiocytes and immunoblasts [4]. Most patients with AITL present with various types of thoracic involvement; however, there are few reports of thoracic images in patients with AITL.

To determine the characteristics of the thoracic involvement observed in patients with AITL, we retrospectively assessed the clinical and radiological data of patients with AITL. The subjects in the present study included five patients (four men and one woman, median age: 74 [67–76] years) who were treated by hematologists between January 2004 and December 2012. All of the subjects were diagnosed pathologically to have AITL using biopsy tissues of lymph nodes, and all of them exhibited abnormal findings in the chest images. Computed tomography (CT) examinations were performed with a high-speed scanner (Hi-Speed Advantage, General Electric Medical Systems,

Abbreviations: AITL, angioimmunoblastic T-cell lymphoma; CT, computed tomography; IL, interleukin

*Corresponding author at: Department of Respiratory Medicine, Fukuoka University Hospital 7-45-1 Nanakuma, Fukuoka-city, Fukuoka, 814-0180, Japan. Tel.: +81 92 801 1011; fax: +81 92 865 6220.
E-mail addresses: hishii@fukuoka-u.ac.jp (H. Ishii), hkushi@oita-u.ac.jp (H. Kushima), komiyakh1@oita-u.ac.jp (K. Komiya), fumitook@oita-u.ac.jp (F. Okada), watanabe@fukuoka-u.ac.jp (K. Watanabe), kadota@oita-u.ac.jp (J.-i. Kadota).

2212-5345/$ - see front matter © 2014 The Japanese Respiratory Society. Published by Elsevier B.V. All rights reserved.
http://dx.doi.org/10.1016/j.resinv.2014.01.001

Table 1 – Patient characteristics and computed tomography (CT) findings.

	Case 1	Case 2	Case 3	Case 4	Case 5
Gender/age	Male/72	Male/76	Female/75	Male/74	Male/67
Symptoms and signs					
Pyrexia	+	+	–	+	+
Swelling of superficial lymph nodes	–	+	+	+	+
Skin rash	–	+	+	–	+
General malaise	+	+	–	–	–
Others [a]	+	–	+	+	+
Laboratory findings					
Elevated lactate dehydrogenase (IU/L)	349	682	919	1026	715
Elevated soluble interleukin-2 receptor (U/mL)	9350	5000	5520	1350	5040
Elevated C-reactive protein (mg/dL)	1.8	8.4	12.8	6.6	5.4
Liver dysfunction	+	–	–	+	+
Anemia	+	–	+	+	–
Outcome from chemotherapies including corticosteroids	Complete remission	Died	Partial remission	Died	Partial remission
CT findings					
Lymphadenopathy [b]	+	+	+	+	+
Bilateral pleural effusion	+	+	+	+	+
Ascites	+	–	–	+	+
Ground glass opacity	+	+	–	–	+
Interlobular septal thickening	+	+	+	+	–
Thickening of bronchovascular bundles	+	+	–	+	–
Consolidation	+	+	–	–	–
Hepatosplenomegaly	+	–	–	+	+

[a] Edema, hepatosplenomegaly, dyspnea, etc.
[b] Hilar, mediastinal, and/or abdominal lymph nodes.

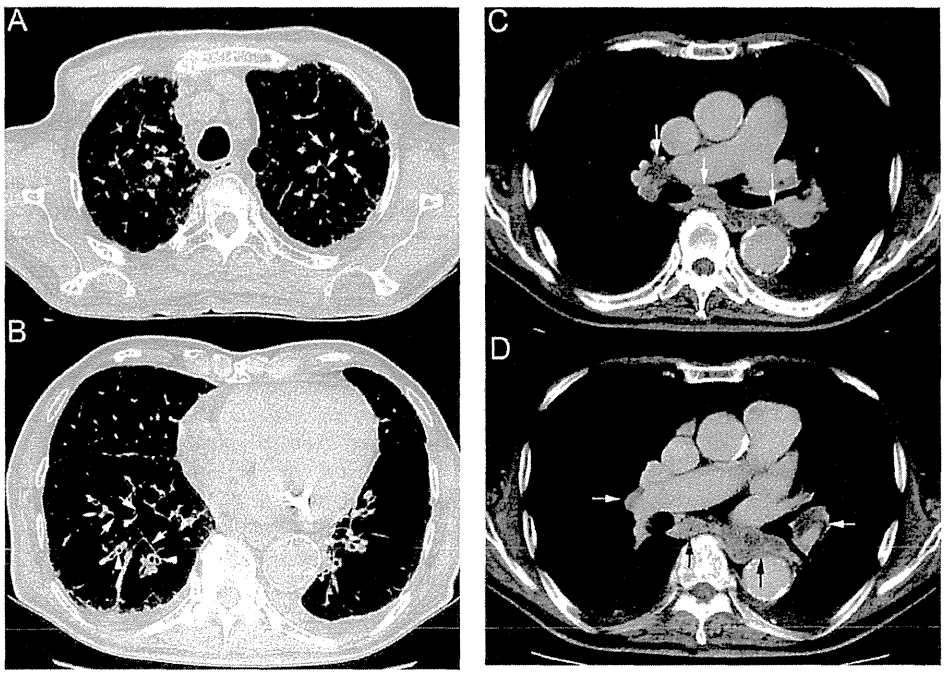

Fig. 1 – Chest computed tomography (CT) scans (1.25-mm thickness) in a representative patient with angioimmunoblastic T-cell lymphoma. The lung window of the CT images (A, B) shows ground-glass opacity, interlobular septal thickening (arrows), and thickening of the bronchovascular bundles (arrowheads). The mediastinal window of the enhanced CT images (C, D) shows mediastinal and hilar lymphadenopathy (arrows) and a bilateral pleural effusion.

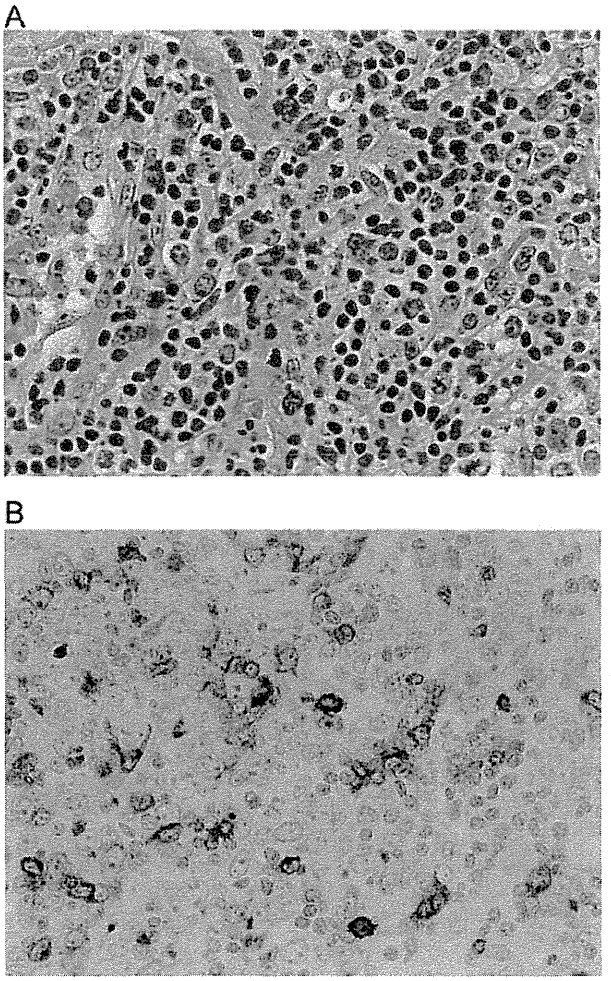

Fig. 2 – A surgical biopsy specimen of the cervical lymph node in a representative patient with angioimmunoblastic T-cell lymphoma shows a mixed infiltrate, including small lymphocytes, histiocytes and plasma cells, with prominent postcapillary venules (A; hematoxylin-eosin staining, original magnification 400 ×). These cells are in part positive for CD10 (B; CD10 staining, 400 ×).

Milwaukee, WI; or X-press unit, Toshiba, Tokyo, Japan). Images were obtained with lung window settings (width, 1500 Hounsfield units [HU]; level, −700 HU) and with mediastinal window settings (width, 400 HU; level, 20–40 HU). All CT scans were obtained during suspended-end inspiration with the patient in the supine position. The ethical review boards of the institutions that contributed cases to this study did not require approval or informed consent for the retrospective review of patient records and images.

The patient characteristics and CT findings are shown in Table 1. The most common signs and symptoms at onset were persistent fever and swelling of the cervical lymph nodes. All of the patients exhibited elevated serum levels of lactate dehydrogenase, soluble interleukin (IL)-2 receptor and C-reactive protein in the laboratory findings. Radiographic findings of the chest (Table 1 and Fig. 1) included mediastinal and hilar lymphadenopathy (observed in 5/5 patients), bilateral pleural effusion (5/5), interlobular septal thickening (4/5), thickening of the bronchovascular bundles (3/5), ground-glass opacity (3/5), consolidation (2/5), and hepatosplenomegaly (3/5). The distribution of ground-glass opacities or thickening of the bronchovascular bundle was varied. These radiographic findings were similar to those in the single case-reports presenting with chest CT [5,6]. The pleural effusion and ascites were exudative fluids but no malignant cells were found, and no patient showed signs or symptoms of cardiac failure. Opportunistic infection was ruled out by serological or microbiological tests in all of the patients. A surgical biopsy specimen of the cervical lymph node in a representative patient is shown in Fig. 2, showing a mixed infiltrate, including small lymphocytes, histiocytes and plasma cells (Fig. 2A). These cells were positive for CD10 (Fig. 2B), CD3, CD4 and CD5, but were negative for L26, CD8, CD30 and UCHL-1 (data not shown). All patients received corticosteroid therapy followed by systemic chemotherapy (e.g., pirarubicin, cyclophosphamide, and etoposide). The thoracic lesions improved simultaneously with the symptoms in response to initial steroid therapy. Two of the patients (cases 2 and 4) attained a temporary partial remission, but died 2–3 years after disease recurrence.

In patients with AITL, the general signs/symptoms and laboratory findings indicating an inflammatory response are thought to be attributed to cytokines (IL-3, IL-5, IL-6, granulocyte/macrophage-colony stimulating factor, and tumor necrosis factor-α), which are directly or indirectly produced by lymphoma cells [1,2]. The thoracic involvement, including lung lesions, pleural effusion and mediastinal lymphadenopathy, may be induced by these cytokines. For this reason, the thoracic lesions temporarily improved in a relatively rapid manner in response to initial steroid therapy. However, the detail of lung pathology of AITL is unknown, because lung biopsy or bronchoalveolar lavage is hardly ever performed owing to the patients' poor general condition. Although the sample size was very small, CT findings of the lung revealed a possible predilection for lymphatic routes but did not show any tendency in the distribution.

Our results indicate that chest physicians and radiologists should be aware that thoracic involvement is frequently seen in patients with AITL, although the disease is a rare type of non-Hodgkin lymphoma.

Conflict of interest

The authors have no conflicts of interest.

Acknowledgments

The authors thank Dr. M. Ogata (Department of Hematology, Oita University Hospital) for the data collection.

REFERENCES

[1] Lachenal F, Berger F, Ghesquieres H, et al. Angioimmunoblastic T-cell lymphoma: clinical and laboratory features at diagnosis in 77 patients. Medicine (Baltimore) 2007;86:282–92.
[2] Iannitto E, Ferreri AJ, Minardi V, et al. Angioimmunoblastic T-cell lymphoma. Crit Rev Oncol Hematol 2008;68:264–71.

[3] Dogan A, Attygalle AD, Kyriakou C. Angioimmunoblastic T-cell lymphoma. Br J Haematol 2003;121:681–91.
[4] Dogan A, Ngu LS, Ng SH, et al. Pathology and clinical features of angioimmunoblastic T-cell lymphoma after successful treatment with thalidomide. Leukemia 2005;19:873–5.
[5] Matsumiya H, Arai A, Nagai A. A case of angioimmunoblastic T-cell lymphoma with interstitial shadow which disappeared after injection of hydrocortisone. Nihon Kokyuki Gakkai Zasshi 2006;44:537–40 ([in Japanese, abstract in English]).
[6] Omura H, Nagata N, Wakamatsu K, et al. Case of angioimmunoblastic T-cell lymphoma with eosinophilia and interstitial shadows. Nihon Kokyuki Gakkai Zasshi 2010;48:831–5 ([in Japanese, abstract in English]).

Histopathology

Histopathology 2015, 66, 545-554. DOI: 10.1111/his.12554

Histological evolution of pleuroparenchymal fibroelastosis

Takako Hirota, Yuji Yoshida, Yasuhiko Kitasato,[1]* Michihiro Yoshimi,[1] Takaomi Koga,[2] Nobuko Tsuruta,[3] Masato Minami,[4] Taishi Harada, Hiroshi Ishii, Masaki Fujita, Kazuki Nabeshima,[5] Nobuhiko Nagata[6] & Kentaro Watanabe

Department of Respiratory Medicine, Fukuoka University School of Medicine, Fukuoka, [1]Department of Respiratory Medicine, [2]Department of Laboratory Medicine, Fukuoka Higashi Medical Centre, National Hospital Organization, Koga, [3]Department of Respiratory Medicine, Hamanomachi Hospital, Fukuoka, [4]Department of General Thoracic Surgery, Osaka University Graduate School of Medicine, Osaka, [5]Department of Pathology, Fukuoka University School of Medicine, and [6]Department of Respiratory Medicine, Fukuoka University Chikushi Hospital, Fukuoka, Japan

Date of submission 12 August 2014
Accepted for publication 15 September 2014
Published online Article Accepted 19 September 2014

Hirota T, Yoshida Y, Kitasato Y, Yoshimi M, Koga T, Tsuruta N, Minami M, Harada T, Ishii H, Fujita M, Nabeshima K, Nagata N & Watanabe K
(2015) Histopathology 66, 545-554. DOI: 10.1111/his.12554

Histological evolution of pleuroparenchymal fibroelastosis

Aims: To investigate the histological evolution in the development of pleuroparenchymal fibroelastosis (PPFE).

Methods and results: We examined four patients who had undergone surgical lung biopsy twice, or who had undergone surgical lung biopsy and had been autopsied, and in whom the histological diagnosis of the first biopsy was not PPFE, but the diagnosis of the second biopsy or of the autopsy was PPFE. The histological patterns of the first biopsy were cellular and fibrotic interstitial pneumonia, cellular interstitial pneumonia (CIP) with organizing pneumonia, CIP with granulomas and acute lung injury in cases 1, 2, 3, and 4, respectively. Septal elastosis was already present in the non-specific interstitial pneumonia-like histology of case 1, but a few additional years were necessary to reach consolidated subpleural fibroelastosis. In case 3, subpleural fibroelastosis was already present in the first biopsy, but only to a small extent. Twelve years later, it was replaced by a long band of fibroelastosis. The septal inflammation and fibrosis and airspace organization observed in the first biopsies were replaced by less cellular subpleural fibroelastosis within 3-12 years.

Conclusions: Interstitial inflammation or acute lung injury may be an initial step in the development of PPFE.

Keywords: acute lung injury, cellular interstitial pneumonia, idiopathic interstitial pneumonia, idiopathic pulmonary fibrosis, organizing pneumonia, pleuroparenchymal fibroelastosis, pulmonary upper lobe fibrosis

Introduction

Pleuroparenchymal fibroelastosis (PPFE) is a unique clinicopathological entity that was first described by Frankel et al.[1] Idiopathic PPFE is now listed as one of the rare idiopathic interstitial pneumonias (IIPs) in the updated classification of IIPs.[2] The concept of PPFE, regarding both clinical features and histopathology, overlaps with that of idiopathic pulmonary upper lobe fibrosis (PULF), which was described initially by Amitani et al.[3] According to that description, idiopathic PULF has been considered to progress slowly, with 10-20 years of presentation. Recently, however, it has been disclosed that PPFE or PULF sometimes progresses rapidly, with a poor prognosis.[4,5] Its pathogenesis appears to be heterogeneous.[6]

Address for correspondence: K Watanabe, Department of Respiratory Medicine, Fukuoka University School of Medicine, Fukuoka 814-0180, Japan. e-mail: watanabe@fukuoka-u.ac.jp
*Present address: Department of Respiratory Medicine, Kurume General Hospital, Kurume 830-0013, Japan

Regarding the evolution of idiopathic pulmonary fibrosis (IPF), it was once widely accepted that end-stage fibrosis is reached via an inflammatory process that starts at the early stage in the lung parenchyma. However, it is now believed that the inflammatory stage is not absolutely necessary for the development of fibrosis; that is, the fibrotic process that follows epithelial injuries could start in the initial stage of the disease, without inflammation.[7] If this is so, what process intervenes in the progression to the established fibroelastosis in PPFE?

In 2013, Ofek et al.[8] published an article that described PPFE as a pathological phenotype of restrictive allograft syndrome following lung transplantation. In that report, the authors showed that PPFE was often associated with diffuse alveolar damage (DAD), and their findings suggested a temporal sequence of DAD followed by the development of PPFE. We hypothesized that not only transplantation-associated PPFE, but also other forms of PPFE, idiopathic or secondary, may have an inflammatory or acute lung injury (ALI) process prior to the development of PPFE. In this article, we present four patients with PPFE who showed features of cellular and fibrotic interstitial pneumonia, cellular interstitial pneumonia (CIP) and an ALI pattern in the first biopsy, and subpleural fibroelastosis in the second biopsy or autopsy. Herein, we discuss the evolution of PPFE regarding the relationships between clinical characteristics and imaging and histological findings.

Materials and methods

We reviewed the medical files of all patients admitted to the Departments of Respiratory Medicine at the Fukuoka University Hospital, National Hospital Organization Fukuoka Higashi Medical Centre and Hamanomachi Hospital from 2006 to 2013, and selected four patients who had undergone surgical lung biopsy twice, or who had undergone surgical lung biopsy and had been autopsied, and in whom the main histological feature of the first biopsy was not PPFE, but the diagnosis of the second biopsy or autopsy was PPFE. Histological findings were reviewed in specimens stained with haematoxylin and eosin and with elastica van Gieson (EVG), to determine the histological differences between first biopsy and second biopsy or autopsy. Clinical data, including serum levels of Krebs von den Lungen-6 (KL-6) and imaging findings, were also reviewed. KL-6, a high molecular mass mucin-like glycoprotein, was originally identified by Kohno et al.,[9] and has been reported to be a sensitive marker for interstitial lung diseases, such as IPF[10] and non-specific interstitial pneumonia (NSIP).[11] Serum levels of KL-6 in PPFE patients are reported to be around the normal upper limit, and tend to be elevated during the course of the disease. Alveolar epithelial cells are likely to be involved in the fibrotic process of the disease, as in other fibrosing or cellular IIPs.[5,6]

The institutional review board of Fukuoka University Hospital approved this retrospective study (#14-5-16).

Results

The clinical characteristics and laboratory data of the four patients are shown in Table 1. Three of the four patients never smoked, and all patients were lean, with a body mass index of 16.9 · 0.8 kg/m^2 (mean · standard error). The serum levels of KL-6 were 510 · 104 U/ml, which is around the normal upper limit.

CASE 1

A 69-year-old man with chest pain visited our hospital. Chest computed tomography (CT) revealed ill-defined nodular opacities attached to the pleura in both the upper and lower lung fields. Six months later, one of the lesions in the right S5 was biopsied by video-assisted thoracoscopic surgery (VATS). Although alveolar architectures were mostly preserved histologically, alveolar septa were diffusely thickened, with fibrosis and a mild degree of mononuclear cell infiltration (Figure 1A,B). The patient was then observed in the outpatient clinic. However, his general condition became gradually worse, with increasing dyspnoea. Multiple nodular opacities with fibrosis on chest CT were also advanced.

Three years and 7 months after the biopsy, the patient was admitted to our hospital. Corticosteroids and cyclophosphamide were administered, but without any beneficial effect. The patient died of rapidly progressive respiratory failure at 41 hospital days, and was autopsied. Autopsy revealed DAD, which seemed to be the direct cause of death. Just beneath the pleura thickened with collagen, there was a band-like gathering of elastic fibres. The border between the elastosis and the normal-appearing lung parenchyma was sharply demarcated (Figure 1C). These features were consistent with those of PPFE. PPFE features were observed in all lobes of both lungs. We reviewed the biopsy specimen, and added

Table 1. Clinical characteristics and laboratory data

	Case 1	Case 2	Case 3	Case 4
Age at first onset (years)	69	56	49	32
Gender	Male	Male	Female	Female
Age at first surgical lung biopsy (years)	69	56	49	32
Age at second surgical lung biopsy (years)	-	-	61	-
Age at autopsy (years)	73	62		35
Smoking status (pack-years)	Never-smoker	Smoker (40)	Never-smoker	Never-smoker
History of pneumothorax	No	No	No	Yes
Past history	NP	NP	NP	IPAH
Family history of interstitial pneumonia	No	No	No	No
Occupational history	Medical technologist	Welder for >25 years	Manager at a sushi bar	No occupational history
Administration of steroids	Yes	Yes	No	Yes
Body mass index (kg/m^2)	15.6	18.9	15.6	17.5
First symptoms	Chest pain	Cough	Chest pain	Exercise dyspnoea
Crackles	Audible	Audible	Not audible	Not audible
Autoantibodies	No	No	No	No
KL-6 (U/ml)	506	793	295	446

IPAH, Post-lung-transplanted state owing to idiopathic pulmonary arterial hypertension; KL-6, Krebs von den Lungen-6; NP, nothing particular.

another specimen stained with EVG, which demonstrated that alveolar septal elastosis was already present (Figure 1D), albeit without band-like consolidated elastosis along the visceral pleura, which is a histological prototype of PPFE, as observed in the autopsy.

CASE 2

A 56-year-old man presenting with cough and mild fever for 2 months underwent right lung biopsies (right S3, S6, and S9) by VATS. Chest CT showed small nodular opacities attached to the pleura in the bilateral apex, and subpleural ground-glass or reticular opacities mainly in the bilateral lower lobes (Figure 2A). The patient had worked as a welder for >25 years, including stainless steel welding for 19 years. He had smoked 20 cigarettes a day for 37 years.

A biopsy specimen taken from S3 showed that alveolar septa were uniformly thickened, with mononuclear cell infiltration; however, the lung architecture was preserved. S6 showed similar microscopic findings. However, in another biopsy specimen taken from S9, alveolar septa were more prominently infiltrated by mononuclear cells. In addition, septal fibrosis and airspace organization were present (Figure 3A,B). The patient was treated with prednisolone and cyclosporine, without a favourable effect. Three years and 5 months after the biopsy, chest CT showed nodular, reticular and linear opacities with bullae distributed mainly in the subpleural areas of bilateral lungs (Figure 2B). The patient's physical condition worsened gradually to severe respiratory failure.

Four years and 2 months after the biopsy, the patient received a left lung transplant from a brain-

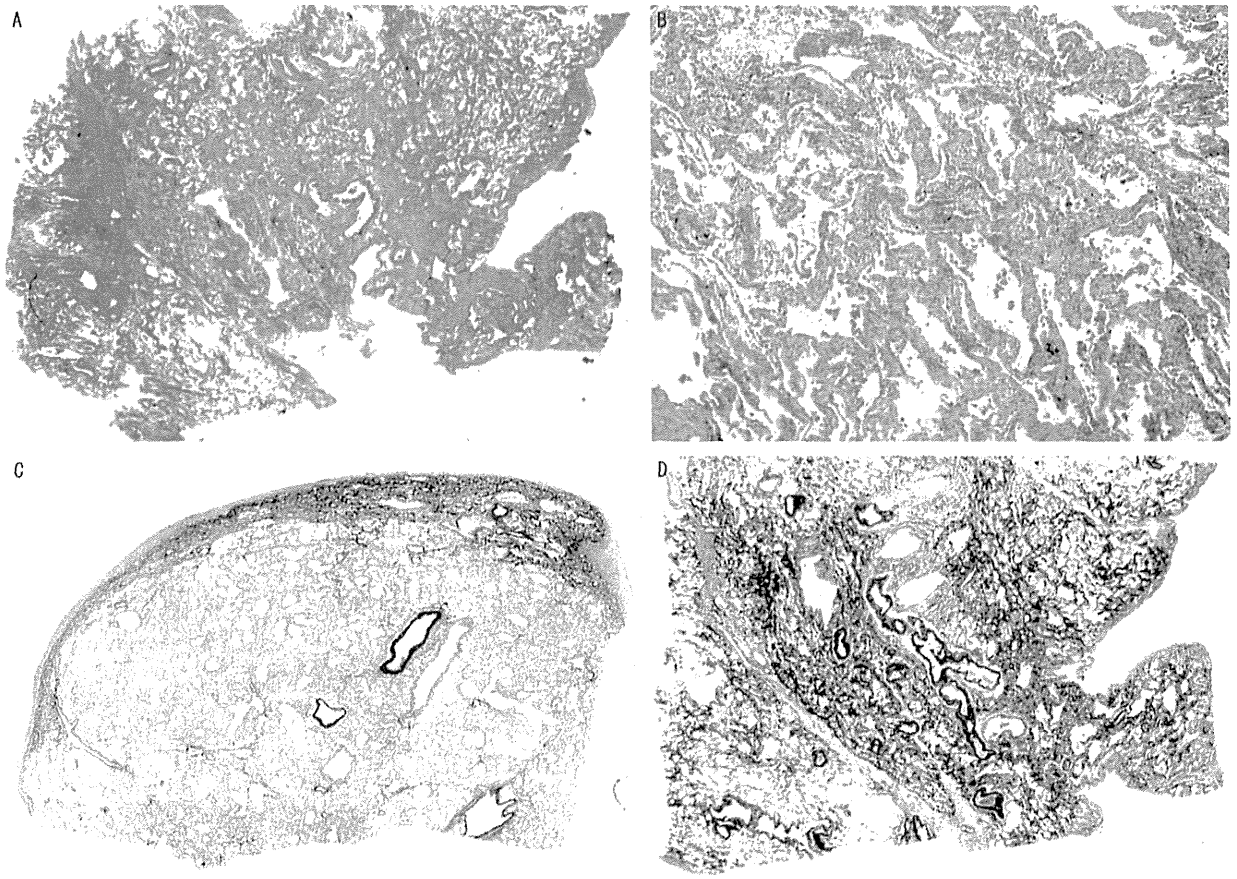

Figure 1. A, A biopsy specimen from right S5 taken from a patient aged 69 years. Alveolar septa were diffusely thickened, with preservation of lung structure [haematoxylin and eosin (H&E)]. B, Alveolar septa were widened with septal fibrosis and a mild degree of inflammatory infiltration (H&E). C, An autopsy specimen taken from the right middle lobe, showing a fibroelastotic band just beneath the fibrously thickened pleura [elastica van Gieson (EVG)]. D, EVG staining of right S5 at biopsy. Lung parenchyma was rich in elastic fibres, with localized aggregates of elastic fibres and alveolar septal elastosis.

dead donor. A histological specimen taken from the superior segment of the left upper lobe showed less cellular fibrosis located in the subpleural area, partly extending inside the lung parenchyma (Figure 3C). EVG staining revealed that the fibrosis was coincident with the aggregation of elastic fibres, together with alveoli filled with mature collagen. Visceral pleurae were locally thickened with collagen (Figure 3D). Other specimens taken from both the left upper and lower lobes showed similar findings. These histological features were compatible with those of PPFE.

The patient's forced expiratory volume in 1 s transiently recovered from 1160 to 1910 ml after the lung transplantation. However, bilateral diffuse ground-glass opacities appeared gradually, and the fibrotic shrinkage of his right lung progressed, with deterioration in his general condition. Two years and 7 months after lung transplantation, he died of respiratory failure and was autopsied. The autopsy confirmed the histological diagnosis of PPFE in the right lung. In addition, diffuse alveolar proteinosis was found. EVG staining was additionally performed for the biopsy specimens, but significant elastosis was not found.

CASE 3

A 56-year-old woman visited our hospital complaining of left chest pain. Chest CT showed irregular pleural thickening or parenchymal nodular opacities attached to the pleura in the bilateral apex. During the subsequent 5-year follow-up without any treatment, nodular opacities gradually expanded, and her body weight decreased by 7 kg over a period of 10 years.

The patient underwent VATS biopsies of the superior and lingular segments of the upper lobe and

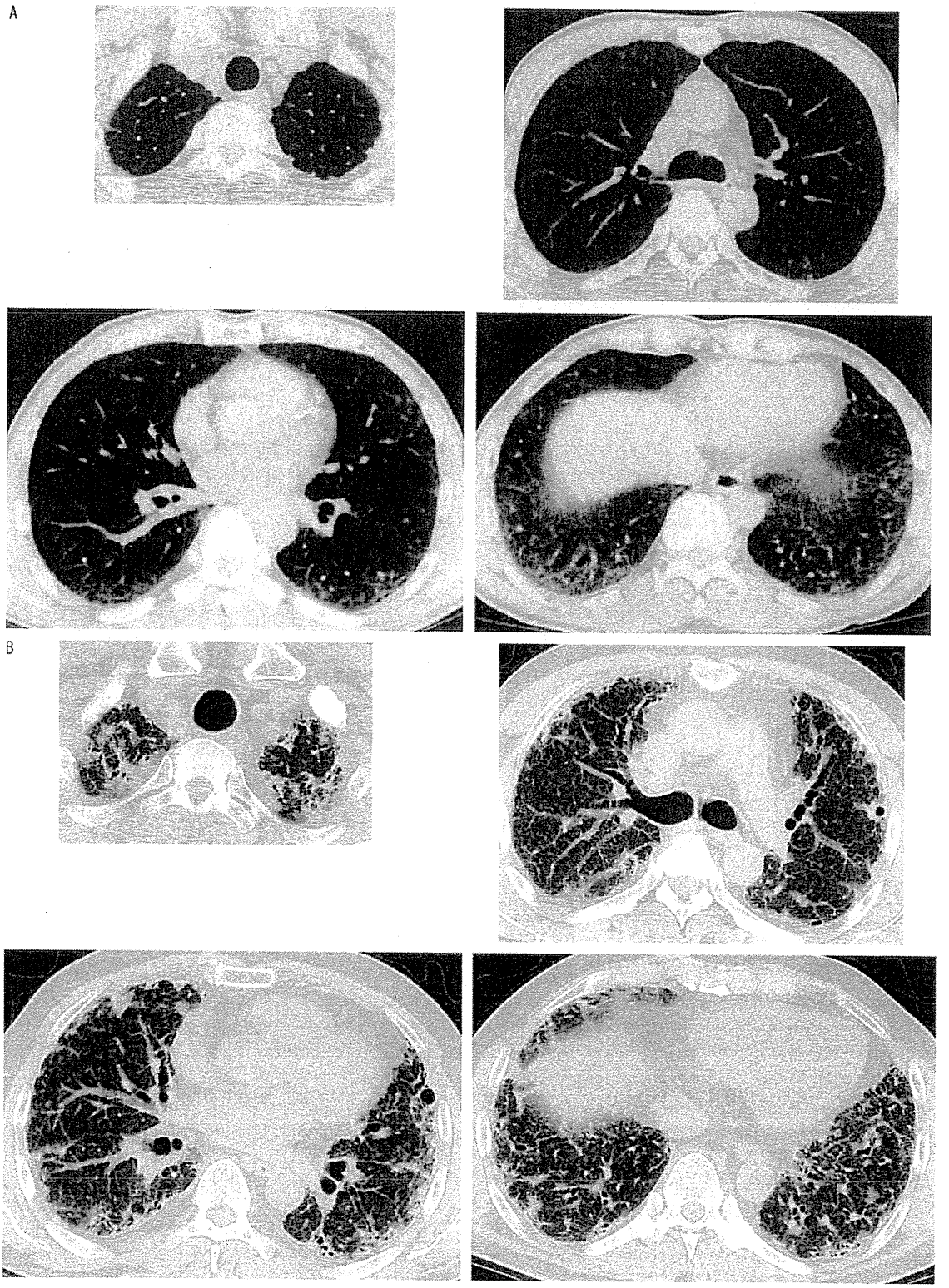

Figure 2. A, Chest computed tomography (CT) scan taken at the age of 56 years, just before the biopsy. B, Chest CT scan taken at the age of 59 years, 3 years and 5 months after the biopsy.

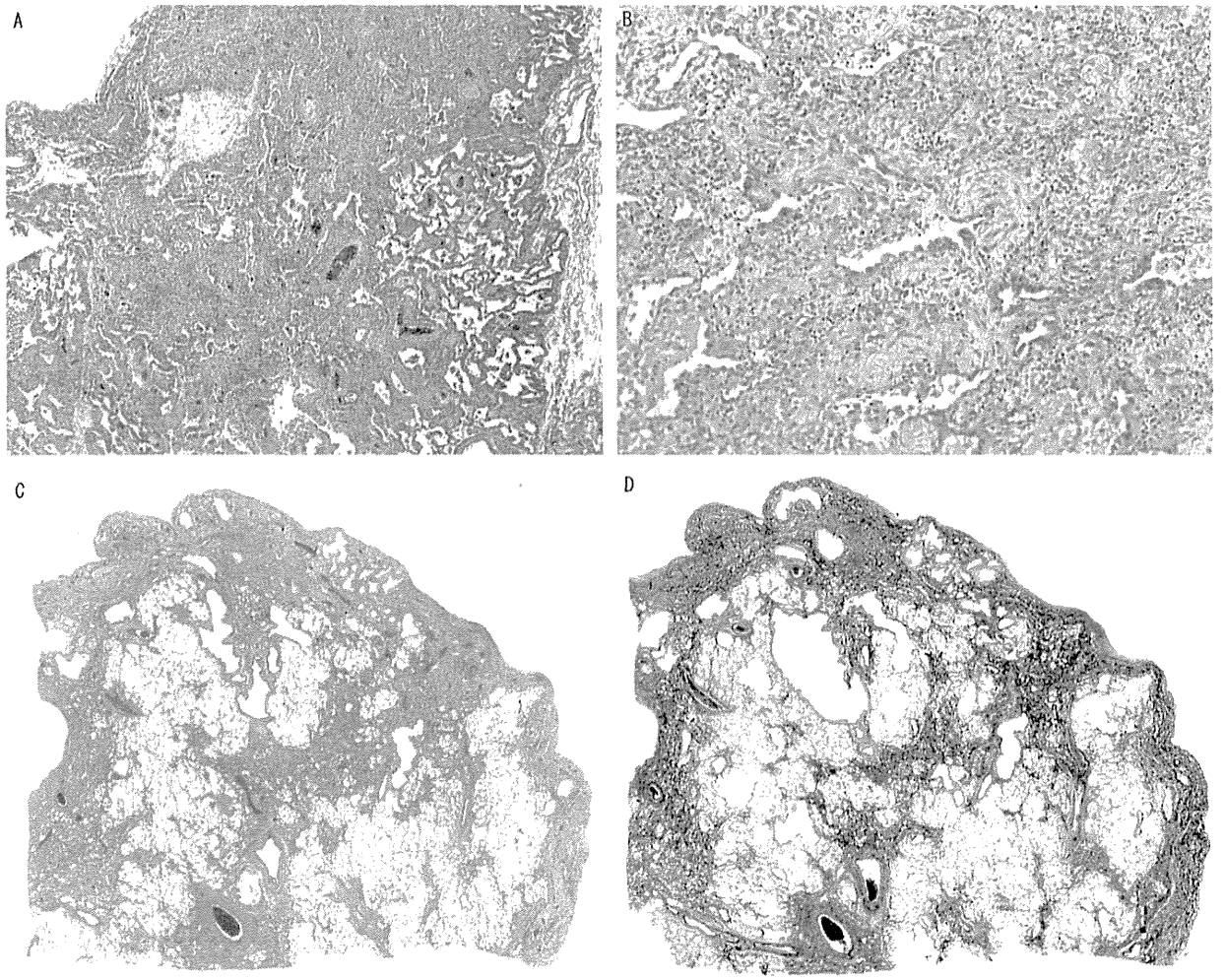

Figure 3. A, A biopsy specimen from right S9 taken from a patient aged 56 years. Alveolar septa were densely infiltrated by mononuclear cells and widened [haematoxylin and eosin (H&E)]. B, Septal fibrosis and airspace organization (H&E). C, A histological specimen taken from the superior segment of the left upper lobe resected for lung transplantation at the age of 60 years (H&E). Lung parenchyma was less cellular than it was at the first biopsy. D, elastica van Gieson staining of the sample depicted in (C), showing subpleural fibroelastosis.

lower lobes of the left lung at the age of 61 years. In the biopsied specimen of the superior segment of the upper lobe, a band-like aggregate of elastic fibres was observed just beneath the pleura, with a sharp demarcation with less-involved lung parenchyma (Figure 4A) and with intra-alveolar collagenous fibrosis around the elastosis. These features were identical to those of PPFE. In the histological specimens taken from the lingular segment and the lower lobe, subpleural elastosis was minimal, with micro-honeycombing associated with the intervening deposition of collagen, consistent with the pattern of usual interstitial pneumonia (UIP) rather than PPFE.

The patient's past history revealed that she had undergone VATS biopsy at the age of 49 years in another hospital. Those biopsy specimens and their paraffin blocks were obtained, and additional histological specimens stained with EVG were prepared to compare the findings of the two biopsies. Biopsied specimens of right S2 showed CIP associated with a localized subpleural band of connective tissue (Figure 4B). Small granulomas with giant cells were sparsely scattered at the border of the connective tissue band (Figure 4C) and in the alveolar septa infiltrated by mononuclear cells. The histological findings of S4 were similar to those of S2, although they were less prominent in cellularity and without subpleural connective tissue bands. Although hypersensitivity pneumonitis was suspected, causative antigens were not identified. The fibrotic band was

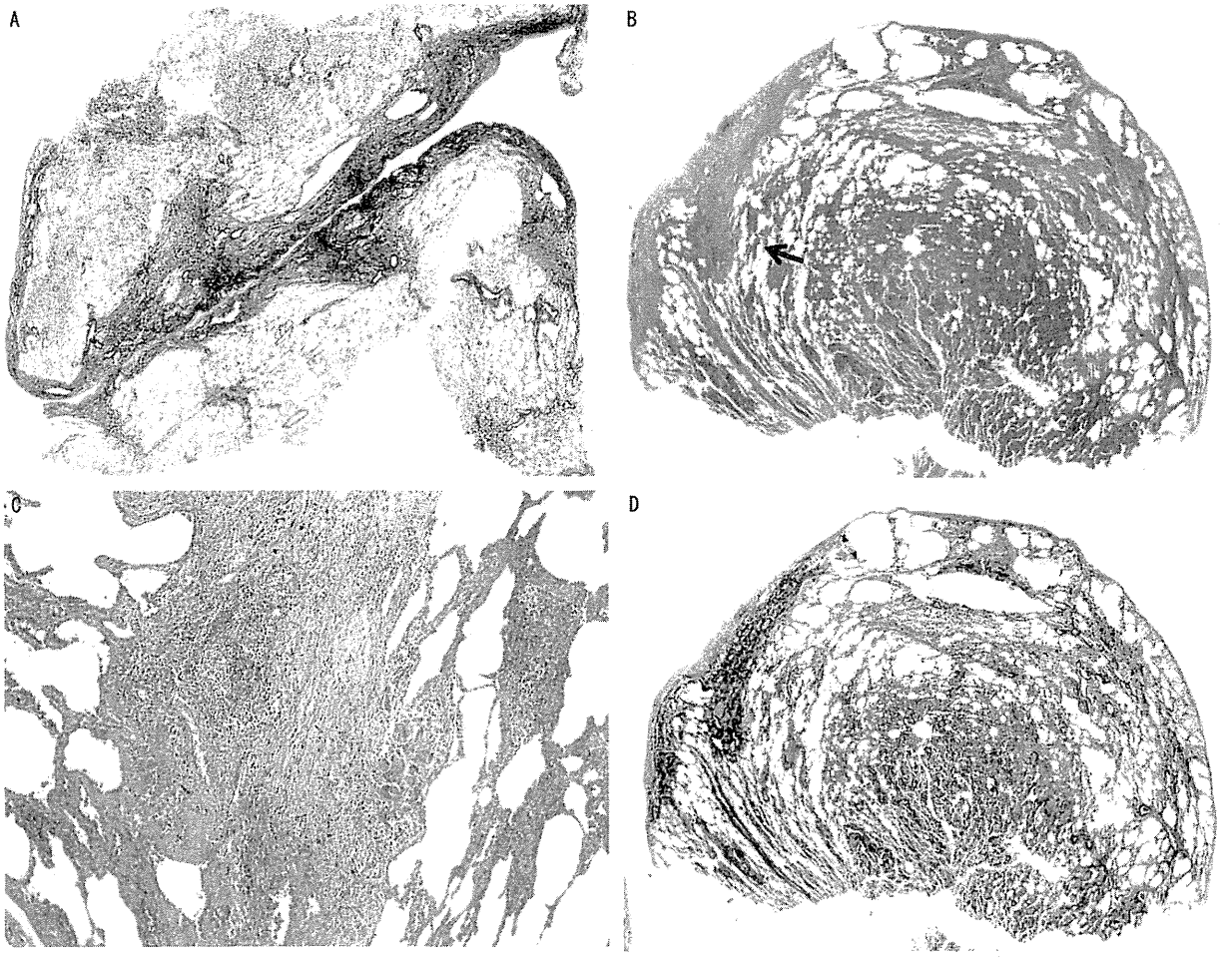

Figure 4. A, A biopsy specimen from the superior segment of the left upper lobe taken from a patient aged 61 years, showing a typical feature of pleuroparenchymal fibroelastosis [elastica van Gieson (EVG)]. B, A biopsy specimen from right S2 taken at the age of 49 years, showing cellular interstitial pneumonia with localized areas of subpleural fibrosis [haematoxylin and eosin (H&E)]. C, Higher magnification of (B) (indicated by a black arrow), showing a granuloma with giant cells adjacent to the subpleural fibrosis (H&E). D, EVG staining of the sample shown in (B), revealing subpleural fibrosis consisting of fibroelastosis.

shown to be fibroelastosis by EVG staining (Figure 4D).

CASE 4

A 30-year-old woman with idiopathic pulmonary arterial hypertension underwent living-donor lung transplantation, receiving a right lower lobe from her younger sister and a left lower lobe from her mother. Twenty-one months after the lung transplantation, the transplanted right lung was surgically biopsied because of progressive dyspnoea and the presence of ground-glass opacities in the upper lung field and interlobular septal thickening with peribronchiolar consolidation in the lower lung field of the right lung on chest CT. Open lung biopsy was performed from the lower parts of the transplanted lung. The biopsy specimen showed massive fibrosis and alveoli with septal thickening (Figure 5A). Organizing connective tissues almost obliterated peripheral airways, intermingled with atypical epithelial cells with an eosinophilic cytoplasm (Figure 5B). These features were consistent with an ALI pattern. In another area, intra-alveolar organizing connective polyps were observed, with CIP (Figure 5C).

In spite of the high doses of corticosteroids administered, the patient's general condition worsened gradually, with increased bilateral interstitial opacities. She died 52 months after lung transplantation. At autopsy, both lungs showed a PPFE pattern (Figure 5D). The autopsy findings have been reported elsewhere.[12] Additional EVG staining for the biopsy specimens failed to reveal significant elastosis.

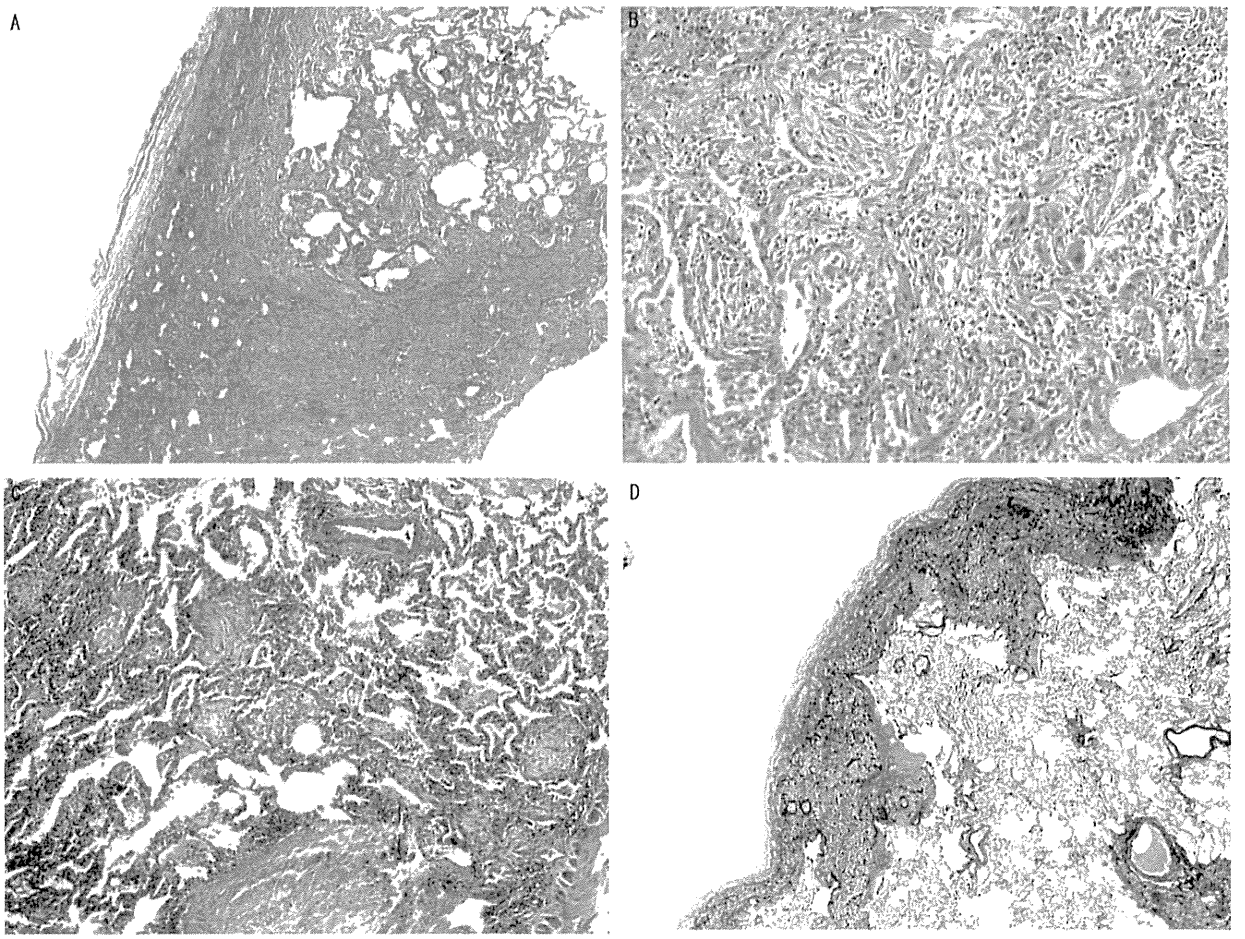

Figure 5. A, A biopsy specimen from the lower part of the transplanted right lung, showing fibrosis and cellular interstitial pneumonia [haematoxylin and eosin (H&E)]. B, Higher-magnification view of the biopsied sample, showing an organizing diffuse alveolar damage pattern (H&E). C, Another area of the biopsied lung at higher magnification, showing an organizing pneumonia pattern (H&E). D, Lower part of the left lung at the autopsy showing subpleural fibroelastosis [elastica van Gieson (EVG)].

Discussion

In this study, we investigated four patients with PPFE confirmed by second biopsy or autopsy; however, the histological features of the first biopsies were considerably different from those of the final biopsies or autopsies.

In case 1, the interval between the biopsy and autopsy was 3 years and 7 months. As the PPFE pattern was observed in all lobes of bilateral lungs at autopsy, it is probable that the NSIP-like pattern observed in the biopsy evolved to subpleural bands of fibroelastosis; that is, alveoli with septal elastosis were gradually compressed, consolidated, and shifted to subpleural areas. Fibroelastosis was already present in the first biopsy, but another few years were required for completion of subpleural fibroelastosis, which is a histological hallmark of PPFE.

In case 2, clinical observations revealed the gradual, but seamless, exacerbation of the disease without imaging improvement, and a PPFE pattern was observed in all specimens taken from the resected left lung. Therefore, it is unlikely that PPFE occurred independently of the histological pattern, i.e. cellular and fibrotic interstitial pneumonia with organizing pneumonia (OP), observed in the biopsy. Prednisolone and cyclosporine seemed to cure the interstitial inflammation, but were unable to prevent disease progression.

Subpleural fibroelastosis was identified in both the first and second biopsies in case 3, but it was more widely distributed in the second biopsy. CIP with granulomas in the first biopsy was not present in the

second biopsy. Although it cannot be denied that CIP with granulomas and PPFE arose independently, granulomas were often found at the edge of fibroelastosis, and were associated with the OP pattern observed in the first biopsy. It is possible that CIP, OP and granulomas were incorporated into the PPFE pattern. Reddy et al.[4] reported a patient with coexistent PPFE and hypersensitivity pneumonitis in the lower lobe. Mycobacterial infection, such as that with Mycobacterium avium-intracellulare, is another possible explanation for the histology. However, repeated sputum examinations failed to identify the organisms. We previously reported a patient with PPFE complicated by M. avium infection.[5]

It is apparent that there was a close relationship between the ALI pattern observed in the biopsy and the PPFE pattern observed in the autopsy in case 4. Clinical observation proved that there was serial exacerbation of symptoms and signs in the period between the biopsy and the autopsy. In addition, repeated examination by CT demonstrated that ground-glass opacities at the apex were transformed into multiple cysts with nodular, reticular and interseptal linear opacities. These findings suggest a temporal sequence of ALI followed by the development of PPFE in the lung-transplanted patient, and were coincident with those observed by Ofek et al.[8]

We have shown in the present study that there is a possible temporal continuity in the histological features from interstitial inflammation and fibrosis or ALI to the development of PPFE. These histological alterations suggest that some inflammatory or lung injury processes might constitute the first step in the occurrence and progression of PPFE.

The most important aspect of our speculation is whether the histology of the autopsies or second biopsies of lungs truly reflects the 'evolutionary process' of the histology of lung tissues obtained in the first biopsy. The combination of upper lobe PPFE and lower lobe UIP[4,5] patterns, and the combination of UIP and NSIP patterns in chronic fibrosing interstitial pneumonia,[2,13] are not rare. As the sampling sites of the second biopsy or autopsy in our patients included the upper lobes, where initial lesions had existed, we think that histology at the second biopsy or autopsy was the result of the 'evolutionary process' of the first biopsy. Serial imaging findings also supported our hypothesis.

The second question is whether such a histological evolution is applicable to all types of PPFE generally. Our study was performed on the basis of clinical and histological analyses of only four patients, which is the major limitation of the present study. As PPFE is a rare interstitial pneumonia, large-scale studies of PPFE patients are necessary to confirm our results.

Honeycomb lung is a non-specific end-stage fibrosis of lung diseases such as IIPs, including UIP.[14,15] Interstitial inflammation and fibrosis with or without granulomas and an ALI pattern as an initial stage might progress to honeycomb lung as an end-stage fibrosis of the interstitial lung diseases. Similarly, we propose subpleural fibroelastosis, considered to be a histological prototype of PPFE, as an end-stage fibrosis of PPFE, idiopathic or secondary, such as transplantation-associated PPFE. As we demonstrated in the present study that interstitial inflammation and fibrosis with or without granulomas and ALI were replaced by subpleural fibroelastosis at various time intervals, we speculate that these lesions could represent an initial step in the development of PPFE.

Pleuroparenchymal fibroelastosis may be a healing reaction. However, PPFE is a distinctive form of chronic scarring in the lung that differs from the common scarring seen in IPF.[16] PPFE lungs contain twice as much elastin as IPF lungs.[17] Also, a histological healing reaction in PPFE does not necessarily mean clinical healing of PPFE. Extensive subpleural elastosis causes serious clinical problems, such as progressive restrictive ventilatory impairment associated with exertional dyspnoea. In that sense, PPFE is a disease entity.

The histological finding of elastosis is not exclusive to PPFE. Other IIPs also have increased amounts of elastic fibres. In the analysis of fibrosing process of IIPs, little attention has been directed to the elastic tissue.[18,19] Idiopathic PPFE is now a member of the rare IIPs.[2] We have to pay more attention to elastosis in IIPs, in order to determine any differences in elastosis between idiopathic PPFE and other IIPs, and to distinguish PPFE as a histological pattern from PPFE as a disease entity. PPFE as a histological pattern, which is true of the apical cap, does not require clinical symptoms and signs. On the other hand, PPFE as a true IIP is a clinical disease with characteristic clinical and physiological findings.

Reddy et al.[4] showed underlying conditions in PPFE: recurrent pulmonary infections, and genetic and autoimmune mechanisms. However, we were unable to identify any of the predisposing causes or diseases described above or a previous history of malignancy[1] (Table 1).

In clinical practice, a diagnosis of PPFE is established only at an advanced stage, when subpleural fibroelastosis develops. At present, we cannot distinguish interstitial inflammation and ALI as initial lesions of PPFE from other inflammatory diseases

until a typical PPFE pattern emerges. PPFE has been widely recognized among pulmonologists since the revised classification of IIPs appeared in 2013.[2] Large-scale and long-term accumulation of patients with PPFE may be needed to elucidate the evolution of PPFE.

Acknowledgements

This work was partly supported by a grant to the Diffuse Lung Diseases Research Group from the Ministry of Health, Labour and Welfare, Japan.

Author contributions

T. Hirota acquisition, analysis and interpretation of data, and drafting and final approval of the manuscript. Y. Yoshida, M. Yoshimi, T. Harada, N. Tsuruta and H. Ishii acquisition of data and final approval of the manuscript. Y. Kitasato and M. Masato acquisition, analysis and interpretation of data, and final approval of the manuscript. T. Koga, K. Nabeshima and N. Nagata analysis and interpretation of data, and final approval of the manuscript. M. Fujita acquisition and analysis of data, and final approval of the manuscript. K. Watanabe conception and design of the study, acquisition, analysis and interpretation of data, and drafting and final approval of the manuscript.

Conflict of interest

The authors declare no conflict of interest.

References

1. Frankel SK, Cool CD, Lynch DA, Brown KK. Idiopathic pleuroparenchymal fibroelastosis. Description of a novel clinicopathologic Entity. Chest 2004; **126**; 2007-2013.
2. Travis WD, Costable U, Hansell DM et al. An Official American Thoracic Society/European Respiratory Society Statement: update of the international multidisciplinary consensus classification of the idiopathic interstitial pneumonias. Am. J. Respir. Crit. Care Med. 2013; **188**; 733-748.
3. Amitani R, Niimi A, Kuze F. Idiopathic pulmonary upper lobe fibrosis. Kokyu 1992; **11**; 693-699.
4. Reddy TL, Tominaga M, Hansell DM et al. Pleuroparenchymal fibroelastosis; a spectrum of histopathological and imaging phenotypes. Eur. Respir. J. 2012; **40**; 377-385.
5. Watanabe K, Nagata N, Kitasato Y et al. Rapid decrease in vital capacity in patients with idiopathic pulmonary upper lobe fibrosis. Respir. Investig. 2012; **50**; 88-97.
6. Watanabe K. Pleuroparenchymal fibroelastosis: its clinical characteristics. Curr. Respir. Med. Rev. 2013; **9**; 229-237.
7. Maher TM, Wells AU, Laurent GL. Idiopathic pulmonary fibrosis: multiple causes and multiple mechanisms? Eur. Respir. J. 2007; **30**; 835-839.
8. Ofek E, Sato M, Saito T et al. Restrictive allograft syndrome post lung transplantation is characterized by pleuroparenchymal fibroelastosis. Mod. Pathol. 2013; **26**; 350-356.
9. Kohno N, Akiyama M, Kyoizumi S et al. A novel method for screening monoclonal antibodies reacting with antigenic determinants on soluble antigens; a reversed indirect-enzyme linked immunosorbent assay (RI-ELISA). Hiroshima J. Med. Sci. 1987; **36**; 319-323.
10. Yokoyama A, Kohno N, Hamada H et al. Circulating KL-6 predicts the outcome of rapidly progressive idiopathic pulmonary fibrosis. Am. J. Respir. Crit. Care Med. 1998; **158** (5 Pt 1); 1680-1684.
11. Ishii H, Mukae H, Kadota J et al. High serum concentrations of surfactant protein A in usual interstitial pneumonia compared with non-specific interstitial pneumonia. Thorax 2003; **58**; 52-57.
12. Hirota T, Fujita M, Matsumoto T et al. Pleuroparenchymal fibroelastosis as a manifestation of chronic lung rejection? Eur. Respir. J. 2013; **41**; 243-245.
13. Flacherty KR, Travis WD, Colby TV et al. Histopathologic variability in usual interstitial and nonspecific interstitial pneumonias. Am. J. Respir. Crit. Care Med. 2001; **164**; 1722-1727.
14. Katzenstein AA ed. Katzenstein and Askin's surgical pathology of non-neoplastic lung disease. 4th ed. Philadelpia: Saunders Elsevier, 2006; 75-78.
15. Corrin B, Nicholson AG. Pathology of the lungs. 3rd ed. London: Churchill Livingstone Elsevier, 2011; 149.
16. Camus P, Th€sen J, Hansell DM et al. Pleuroparenchymal fibroelastosis: one more walk on the wild side of drugs? Eur. Respir. J. 2014; **44**; 289-296.
17. Enomoto N, Kusagaya H, Oyama Y et al. Quantitative analysis of lung elastic fibers in idiopathic pleuroparenchymal fibroelastosis (IPPFE): comparison of clinical, radiological, and pathological findings with those of idiopathic pulmonary fibrosis (IPF). BMC Pulm. Med. 2014; **14**; 91.
18. Negri EM, Montes GS, Saldiva PHN et al. Architectural remodelling in acute and chronic interstitial lung disease: fibrosis or fibroelastosis? Histopathology 2000; **37**; 393-401.
19. Rozin GF, Gomes MM, Parra ER et al. Collagen and elastic system in the remodeling process of major types of idiopathic interstitial pneumonia (IIP). Histopathology 2005; **46**; 413-421.

Clinical Immunology (2013) 149, 357–364

available at www.sciencedirect.com

Clinical Immunology

www.elsevier.com/locate/yclim

Light chain (κ/λ) ratio of GM-CSF autoantibodies is associated with disease severity in autoimmune pulmonary alveolar proteinosis☆☆

Takahito Nei[a,b], Shinya Urano[a], Yuko Itoh[a], Nobutaka Kitamura[c], Atsushi Hashimoto[a], Takahiro Tanaka[a], Natsuki Motoi[a], Chinatsu Kaneko[a], Ryushi Tazawa[a], Kazuhide Nakagaki[d], Toru Arai[e], Yoshikazu Inoue[e], Koh Nakata[a,*]

[a] *Bioscience Medical Research Center, Niigata University Medical and Dental Hospital, Niigata, Japan*
[b] *Department of Respiratory Medicine, Nippon Medical School, Tokyo, Japan*
[c] *Department of Medical Informatics, Niigata University Medical and Dental Hospital, Niigata, Japan*
[d] *Laboratory of Infectious Diseases and Immunology, College of Veterinary Medicine, Nippon Veterinary and Life Science University, Tokyo, Japan*
[e] *Department of Diffuse Lung Diseases and Respiratory Failure, National Hospital Organization Kinki-Chuo Chest Medical Center, Japan*

Received 15 June 2013; accepted with revision 3 October 2013
Available online 11 October 2013

KEYWORDS
Pulmonary alveolar proteinosis;
Anti-GM-CSF autoantibody;
Light chain ratio

Abstract Previous studies demonstrated that antigranulocyte colony-stimulating factor autoantibody (GMAb) was consistently present in patients with autoimmune pulmonary alveolar proteinosis (aPAP), and, thus, represented candidature as a reliable diagnostic marker. However, our large cohort study suggested that the concentration of this antibody was not correlated with disease severity in patients. We found that the κ/λ ratio of GMAb was significantly correlated with the degree of hypoxemia. The proportion of λ-type GMAb per total

☆☆ This work was partially supported by a grant from Category B24390208 and B12023059 from the Japan Society for the Promotion of Science. This research was also supported by a grant from the Ministry of Health, Labour, and Welfare (H24, Nanchitou-ippan-035 and H24 Rinken Sui-003).

* Corresponding author at: Bioscience Medical Research Center, Niigata University Medical and Dental Hospital, 1-754 Asahimachi-dori, Niigata 951-8520, Japan. Fax: +81 25 227 0377.
E-mail addresses: takahitonei@gmail.com (T. Nei), hoshisagashi@yahoo.co.jp (S. Urano), y-itoh@med.niigata-u.ac.jp (Y. Itoh), nktmr@m12.alpha-net.ne.jp (N. Kitamura), noiredge2007@yahoo.co.jp (A. Hashimoto), belltatnk@gmail.com (T. Tanaka), natsumo87@gmail.com (N. Motoi), kanegon0719@gmail.com (C. Kaneko), ryushi@med.niigata-u.ac.jp (R. Tazawa), nakagaki@nvlu.ac.jp (K. Nakagaki), to-arai@kch.hosp.go.jp (T. Arai), GlichiYi@aol.com (Y. Inoue), radical@med.niigata-u.ac.jp (K. Nakata).

http://dx.doi.org/10.1016/j.clim.2013.10.002

λ-type IgG was significantly higher in severely affected patients than those in mildly affected patients, but the proportion of κ-type was unchanged. The κ/λ ratio was significantly correlated with both KL-6 and SP-D, which have been previously reported as disease severity markers. Thus, the light chain isotype usage of GMAb may not only be associated with the severity of aPAP, but may also represent a useful disease severity marker.

1. Introduction

Detection of granulocyte macrophage-colony stimulating factor (GM-CSF) autoantibody (GMAb) is known to be an excellent test with almost 100% sensitivity and specificity for the serological diagnosis of autoimmune pulmonary alveolar proteinosis (aPAP), which comprises 90% of all acquired PAP cases. This indicates its potential value in the routine clinical diagnosis of the disease; however, the test has neither approval nor commercial availability for clinical use [1]. On the other hand, our previous report demonstrated that serum GMAb levels were not correlated with the degree of hypoxemia [2] (according to disease severity score; partial pressure of oxygen in arterial blood, PaO_2; and alveolar–arterial oxygen difference, $AaDO_2$), but were moderately correlated with serum surfactant protein-A, -D, Krebs von den Lungen (KL)-6, and carcinoembryonic antigen (CEA) levels [1]. Because the autoantibodies were polyclonal, thereby recognizing multiple target epitopes on GM-CSF molecules with variable binding avidity, the loss of GM-CSF bioactivity in the lungs of patients with aPAP was thought to be affected not only by the concentration but also by multiple properties of GMAb such as binding avidity, neutralizing capacity, or targeting epitope. Thus, no characteristic correlation has been demonstrated between the properties of GMAb and the degree of hypoxemia.

Each B lymphocyte expresses only one isotype of light chain, κ or λ, which remains fixed for the life of the B lymphocyte. While immunoglobulin synthesis is matured and continually stimulated, the λ chain immunoglobulin concentration reaches a plateau by one year after birth and is maintained throughout the child's life [3]. On the other hand, the concentration of the κ chain, which increases gradually until 20 years of age, reflects the concentration of immunoglobulins as a whole [3,4]. The κ/λ ratio of immunoglobulin in normal adults ranges from 0.85 to 1.86 [5,6], from which it then becomes divergent in patients with monoclonal gammopathy or some autoimmune diseases. Studies suggest a selective preference for either κ- or λ-light chains in autoantibody formation, such as rheumatoid factor (RF) [7,8], anti-cardiolipin antibodies [9], anti-neutrophil antibodies [10], several thyroid-stimulating antibodies [11,12], anti-lamin B antibody [13], and circulating immune complexes in juvenile idiopathic arthritis [14]. Thus, measuring κ/λ ratios in some autoantibodies may be useful to identify the state of activation of B cells involved in some autoimmune diseases. Studies suggest selective preference for either κ or λ chains in autoantibody formation.

During a previous study on characterization of GMAb in patients with aPAP in comparison to pharmaceutical immunoglobulin (IVIG), which was produced from pooled normal sera of more than 1000 normal subjects, we measured concentrations, binding avidities, and κ/λ ratios of GMAb. We noticed that the κ/λ ratio was much higher for GMAb than for whole IgG in both IVIG and aPAP groups, but it decreased as the disease severity of aPAP increased. The aim of this study was to assess the potential use of the κ/λ ratio as a disease severity marker in aPAP. In addition, we discuss the possibility that a selective preference in light chain isotype usage might be associated with the pathogenesis of aPAP.

2. Materials and methods

2.1. Subjects

Forty-six patients with aPAP were enrolled in this study. All patients were diagnosed with PAP by computed tomography findings and lung biopsy or bronchoalveolar lavage findings, and diagnosis was confirmed by the existence of GM-CSF autoantibodies in sera according to the diagnostic criteria (http://www.pap-guide.jp/en/). The median age, gender, proportion of symptomatic individuals, mean arterial blood oxygen pressure, and mean percent vital capacity were comparable to those in our previous large cohort study [2]. All serum and plasma samples were gathered in our institution to measure the level of GM-CSF autoantibodies after written informed consent to collect samples. All participants provided written informed consent; minors provided consent in accordance with the Declaration of Helsinki. Healthy volunteers were also enrolled into the study as healthy subjects (HS) after agreement with written informed consent. All patients with aPAP were categorized by disease severity score (DSS) at enrollment, as previously described [2], from least severe (DSS-1) to most severe (DSS-5).

2.2. Pharmaceutical immunoglobulin (IVIG)

Eight different batches of pharmaceutically-prepared immunoglobulin, Venoglobulin-IH™, were kindly provided by Mitsubishi Pharma Corporation (Tokyo, Japan).

2.3. Enzyme-linked immunosorbent assay (ELISA)

2.3.1. Whole IgG

The serum concentration of whole IgG was measured by using a human IgG ELISA quantitation kit (Bethyl, Montgomery, TX, USA) according to the manufacturer's instructions.

2.4. GM-CSF autoantibody

Serum and culture medium GM-CSF autoantibody levels were measured using direct ELISA as previously reported [15–17]. In brief, micro-ELISA plates (Maxisorp™ flat-bottom, clear, 96-well plates; Nunc, Roskilde, Denmark) were coated with

recombinant human (rh) GM-CSF produced in *Saccharomyces cerevisiae* (Leukine™, sarglamostim; Genzyme, Boston, MA, USA) at 2 μg/ml with phosphate-buffered saline (PBS) at 4 °C overnight. After washing with PBS containing 0.1% Tween™-T (0.1% PBS-T) (MP Biomedicals, Solon, OH, USA), plates were stabilized with blocking solution (Stabilcoat™, SurModics, Eden Prairie, MN, USA) for 1 h at room temperature. Standard human monoclonal GM-CSF autoantibodies with λ light chain isotypes were kindly provided by Dr. Kenzo Takada (Evec Co. Ltd., Sapporo, Japan). Standard GM-CSF autoantibody was diluted in PBS containing 1% bovine serum albumin (1% BSA/PBS) and was used as a standard for antibody measurement. Serum and plasma samples were diluted into 1% BSA/PBS at a 3000-fold dilution, and a volume of 50 μl of prepared samples and standard was transferred to plates. After keeping plates at room temperature for 1 h and washing with 0.1% PBS-T, autoantibodies captured by rhGM-CSF were detected by peroxidase-labeled anti-human Fcγ, Fcμ, or Fcα antibody (Dako Corporation, Carpinteria, CA, USA). After washing, color was developed using tetramethylbenzidine (TMB) solution, and the absorbance was measured at 450 nm.

2.5. Light chain assay

Based on the same ELISA method as above, peroxidase-conjugated anti-human lambda light chain antibody (Bethyl) was used for antibody detection. As the human monoclonal antibody had λ-chains, we used this as the standard for λ-type GMAb. The κ-type GMAb level was calculated by subtraction of each λ-type GMAb level from the GMAb level.

2.6. Binding avidity

The rhGM-CSF (Leukine®) was dialyzed against PBS (pH 7.4) and biotinylated using the NHS-PEO-biotin kit and monomeric avidin kit (Pierce Biotech, Rockford, IL, USA) according to the manufacturer's instructions. The purity of biotinylated GM-CSF (bGM-CSF) was almost 100%. For estimation of binding avidity, the serum GMAb concentration was fixed at 0.685 nM (100 ng/ml) in every assay and was incubated with various concentrations of bGM-CSF (0–1.25 nM) at 4 °C for 1 h and then transferred into a 96-well plate, which was previously coated with 1 μg/ml of anti-human IgG (Bethyl). The bound bGM-CSF was reacted with streptavidin-peroxidase. Then, the reactant was colored with TMB solution, and the OD (at 450 nm) was measured. Based on Lineweaver–Burk plots of the concentration of bGM-CSF and OD values, the average binding dissociation constant (Kd) was determined from the concentration of bGM-CSF at 50% of the maximal OD value.

2.7. Statistical analysis

Numerical data were evaluated for a normal distribution using Shapiro–Wilk tests and for equal variance using Levine median tests. Parametric data are presented as means (±SE), and non-parametric data are presented as medians and ranges. Nonparametric data were compared with the use of the Mann–Whitney *U* test (for two groups, non-paired), or Wilcoxon signed-rank test (for two groups, paired). Correlation coefficients were obtained using the Spearman's correlation method. All tests were two-sided, and *P*-values b 0.05 were considered to indicate statistical significance. Data were analyzed by using JMP (8.0.1) software (SAS, Cary, NC). Figures were made by Stat View (v. 5.0) (SAS, Cary, NC) and Microsoft Power Point (Microsoft, Seattle, WA).

3. Results

3.1. Demographic features of the study subjects

Forty-six patients with positive serum GMAb and pathologically-proven PAP were enrolled in this study. The demographic features, including age, gender, symptoms, arterial blood gas analysis, pulmonary function tests (percent vital capacity, %VC; percent forced expiratory volume in one second, $\%FEV_{1.0}$, and, percent diffusing capacity for carbon monoxide, $\%DL_{CO}$), DSS, and serum markers (KL-6 and SP-D) (Table 1) in this group were similar to those of the 223 participants in our previous cross-sectional, large cohort study [2], indicating that patients in the present study had similar backgrounds to the general demographic features of aPAP in Japan. The median PaO_2 was 67.5 mm Hg, and the numbers of patients in each DSS were 11, 6, 18, 8, and 3 for DSS 1 to 5, respectively, with a mean score of 2.7 ± 1.2.

3.2. Association of GMAb concentrations and binding avidities with disease severity

To assess the correlation of GMAb properties with disease severity, we first investigated the concentration and its proportion to whole IgG in the sera of patients with aPAP as compared to IVIG. As shown in Fig. 1A, the concentrations of IgG isotype GMAb were higher than 3.0 μg/ml in all patients, with a mean value of 46.7 ± 34.1 μg/ml, whereas the levels were less than 3.0 μg/ml for IVIG (2.21 ± 0.38 μg/ml, n = 8). The mean percentage of GMAb per total IgG was 21.7-fold higher in aPAP than in IVIG (*P* b 0.0001, Fig. 1B). "Both the concentrations and the percentages did not correlate with the degree of hypoxemia (i.e., PaO_2, $AaDO_2$, and DSS) (Supplemental Table 1).

Thus, we confirmed our previous results in a large cohort study [2] using a different set of samples in this study.

Then, we evaluated the correlation of binding avidity with disease severity. As the concentration of GMAb increased, the avidity to recombinant human GM-CSF was remarkably variable among the patients, with a mean value of 0.48 nM (Fig. 1C). The mean avidity value was higher in IVIG than those in aPAP patients (*P* b 0.05). As the binding avidity of antibodies is generally thought to reflect the frequency and intensity of ligand stimulation, we considered that the avidity of GMAb in aPAP patients might be associated with disease severity. However, the avidity correlated with none of the parameters regarding the degree of hypoxemia (Supplemental Table 1).

Our previous study demonstrated that serum biomarkers KL-6, SP-D, and pulmonary functions correlated with disease severity [2]. Similarly, we confirmed these results using the present data set. Both KL-6 and SP-D were correlated moderately to strongly with the degree of hypoxemia as shown in Supplemental Table 1. Of pulmonary function data, percent vital capacity (%VC) and percent diffusing capacity